Published in final edited form as:
Biomaterials. 2011 November ; 32(32): 8077–8086. doi:10.1016/j.biomaterials.2011.07.029.

Comparison of polymer scaffolds in rat spinal cord: A step toward quantitative assessment of combinatorial approaches to spinal cord repair

Bingkun K. Chen, MD, PhD[1], **Andrew M. Knight, PhD**[1], **Nicolas N. Madigan, MB, BCh**[1], **LouAnn Gross**[1], **Mahrokh Dadsetan, PhD**[2], **Jarred J Nesbitt**[1], **Gemma E. Rooney, PhD**[1], **Bradford L. Currier, MD**[2], **Michael J. Yaszemski, MD, PhD**[2], **Robert J. Spinner, MD**[3], and **Anthony J. Windebank, MD**[1]

[1]Department of Neurology, Mayo Clinic, Rochester, Minnesota

[2]Department of Orthopedic Surgery, Mayo Clinic, Rochester, Minnesota

[3]Department of Neurosurgery, Mayo Clinic, Rochester, Minnesota

Abstract

The transected rat thoracic ($T_{9/10}$) spinal cord model is a platform for quantitatively compa0ring biodegradable polymer scaffolds. Schwann cell-loaded scaffolds constructed from poly (lactic co-glycolic acid) (PLGA), poly(ε-caprolactone fumarate) (PCLF), oligo(polyethylene glycol) fumarate (OPF) hydrogel or positively charged OPF (OPF+) hydrogel were implanted into the model. We demonstrated that the mechanical properties (3-point bending and stiffness) of OPF and OPF+ hydrogels closely resembled rat spinal cord. After one month, tissues were harvested and analyzed by morphometry of neurofilament-stained sections at rostral, midlevel, and caudal scaffold. All polymers supported axonal growth. Significantly higher numbers of axons were found in PCLF ($P < 0.01$) and OPF+ ($P < 0.05$) groups, compared to that of the PLGA group. OPF + polymers showed more centrally distributed axonal regeneration within the channels while other polymers (PLGA, PCLF and OPF) tended to show more evenly dispersed axons within the channels. The centralized distribution was associated with significantly more axons regenerating ($P < 0.05$). Volume of scar and cyst rostral and caudal to the implanted scaffold was measured and compared. There were significantly smaller cyst volumes in PLGA compared to PCLF groups. The model provides a quantitative basis for assessing individual and combined tissue engineering strategies.

Keywords

OPF; PLGA; PCLF; axon regeneration; spinal cord injury; Schwann cell

Corresponding Author: Anthony J. Windebank, M.D., Department of Neurology, Mayo Clinic, 200 First Street SW, Rochester, MN 55905., windebank.anthony@mayo.edu.

Introduction

The destruction and atrophy of axons in conjunction with glial scar and cyst formation form a physical barrier restricting axonal regeneration after spinal cord injury [1]. In completely destructive injuries, there are two ways to reconnect links and functions below the injured area: bypassing the injured site or rebuilding functional tissue within the cysts and scars. Neuronal survival, axonal growth and remyelination as well as reconnection across the injured site are required for the spinal cord repair with the help of the bridging grafts [2].

Spinal cord repair is complex and will require combining multiple modalities including extracellular architecture, surface or molecular contact guidance cues and appropriate cells. Tissue engineering offers the possibility of bringing polymer chemistry and cellular neurobiology in developing new therapeutic strategies for patients [3–5]. In this context, it is critical to develop model systems that allow deconstruction of the process and quantification of the contributions of individual components to successful regeneration. Polymer scaffolds for neural tissue engineering provide three-dimensional support mimicking the architecture of the extracellular matrix (ECM) for in vitro and in vivo cell growth and tissue construction [6, 7]. We have previously studied a number of different biodegradable synthetic polymers [8–22] and their role as potential scaffolds in nervous system repair in both cell and animal models.

Many cell types have been studied in animal models of spinal cord injury, including schwann cells (SCs) [23]. SCs supported regeneration both in peripheral and central nervous systems, and they have specifically been shown to promote axonal regeneration in the model of spinal cord injury [13, 23–26]. Recently we demonstrated schwann cell survival for up to 6 weeks in rats after implantation of a multichannel polymer scaffold in a complete transection study. We directly compared cell types, and found that schwann cells exhibited a higher capacity than stem cell neurospheres to promote axonal regeneration in the transected spinal cord [14]. This study used a scaffold made from PLGA, a polymer used clinically in absorbable suture material, which has been studied extensively in our laboratory [17]. While schwann cells are a promising cell type, the optimal polymer type for delivery of these cells to the injured cord remains unknown. PLGA is approved for human use by the Food and Drug Administration (FDA) and is used in many clinical applications. PCLF is a novel biodegradable polymer that has been developed for directed bone and nerve regeneration. This copolymer is self-cross-linkable and biocompatible. Scaffolds fabricated from this material can serve as support for neural tissue engineering applications [16]. OPF is a third polymer type under development within our collaborative group. OPF is a PEG based macromer incorporating a fumarate moiety that is photo-cross-linked to form a biocompatible and biodegradable hydrogel [27]. OPF can be copolymerized with [2-(methacryloyloxy) ethyl]-trimethylammonium chloride (MAETAC) to produce a positively charged hydrogel (OPF+). We have shown that the positively charged substrate enhanced neuronal cell attachment, SC migration and axonal myelination *in vitro* [12], making this an attractive candidate as scaffold material *in vivo*.

In the present study, we describe a model system that allows comparison between four different polymers (PLGA, PCLF, OPF and OPF+) used to construct biodegradable, multichannel scaffold for implantation with SCs. The degree of axonal regeneration is quantitatively compared across the groups by means of neurofilament staining of transverse sections and counting of axons at multiple levels through the scaffold.

Materials and methods

2.1. Scaffold manufacturing

PLGA scaffolds with 7 parallel channels (660-μm diameter) were fabricated by injection molding and solvent evaporation as previously described [17]. OPF and OPF+ were synthesized and fabricated as nerve conduits according to the previously published methods (Scheme 1) [12, 16, 27–33]. PCLF with 1% Irgacure 819 (Ciba Specialty Chemicals Corp, New York) formulation was injected into scaffold molds that consisted of a glass tube with seven evenly spaced stainless steel rods coated with Ease Release 2000 (Mann Release Technologies, Easton, PA). After treatment under UV light (MRC 58 Multiple Ray Lamp, UVP, Upland, CA) for one hour the PCLF scaffold tube was cleaned and 'etched' in 3 changes of acetone over 48 hours, before being vacuum dried for 24 hours [16, 34]. Scaffolds were cut into 2-mm lengths and washed in serial dilutions of absolute alcohol for 30 minutes with mild shaking for sterilization and elimination of residual mold lubricant. PLGA scaffolds were dried by vacuum for 24 hours for removing the alcohol, sealed in sterilized glass tubes and then kept dried at 4°C until furt her use. PCLF and OPF scaffolds were washed 3 times in sterile PBS over a couple of hours after incubating in 80% ETOH for 30 minutes.

2.2. Mechanical property of polymer scaffolds

Three-point bending and compression modulus of PCLF, OPF, OPF+ and PLGA conduits were measured using a dynamic mechanical analyzer (DMA2980, TA instruments) at room temperature. Three-point bending in a dynamic mechanical analyzer was used to measure flexural modulus of conduits as previously described [34]. Freshly isolated spinal cord from rat was harvested and compared in the same system within 15 minutes of isolation. Polymer conduits had an average outer diameter of 2.2 mm for OPF conduits, 2.6 mm for OPF+ conduits, 2.4 mm for PLGA conduits, 3.03 mm for PCLF conduits, and a fixed length of 8.5 mm. Six specimens were measured and averaged for each sample. For measurements of compression, modulus was measured on the conduits with thickness of 2 mm as used in transected spinal cord. The test was performed under load control, where load was applied at a rate of 4 N/min. Stress and strain data collected during testing were plotted, and the storage modulus was determined as the slope of the linear region of the stress versus strain curve, as previously described [35].

2.3. Primary schwann cell isolation and culture

Primary neonatal schwann cells were obtained from sciatic nerves of P4 rats [36, 37]. Pups were humanely euthanized by intraperitoneal injection of sodium pentobarbital (Sleepaway, Fort Dodge Animal Health, Fort Dodge, Iowa). Under aseptic conditions, sciatic nerves were surgically isolated and removed from the both legs. Harvested nerves were pooled. The connective tissues and epineurium were removed. Sciatic nerves were cut into 1-mm^3 pieces, and then digested enzymatically for 45 minutes with 0.25% trypsin EDTA (Mediatech Inc, Herndon, Virginia) and 0.03% collagenase (Sigma, St. Louis, Missouri) in Hank's balanced salt solution (Gibco, Grand Island, New York). After digestive treatment and mechanical dissociation, cells were pelleted for 5 minutes at 800 rpm. Cells were re-suspended in 5 ml of DMEM/F12 medium containing 10% fetal bovine serum and 100 units/ml penicillin/streptomycin (Gibco, Grand Island, New York) following removal of the supernatant. Then the cells were plated onto 35-mm laminin-coated dishes (Falcon; Becton Dickinson Labware, Franklin Lakes, New Jersey) and incubated at 37°C in 5% CO_2 for 48 hours as previously described [13].

2.4. Scaffold loading

Schwann cells were detached from dishes by incubating with trypsin-EDTA for 2 minutes and suspended at a density of 5×10^5 cells/μL in chilled Matrigel™ (BD Biosciences, San Jose, CA) [38, 39]. Each single channel of the 7-channeled scaffold was loaded with cells under a microscope at 4°C by using a gel-loading pipette tip. The interior volume of each single channel was 0.67 μL, reaching an ultimate loading of 2.4×10^6 cells per scaffold. Loading efficiency was evaluated and ascertained by immediately flushing out cells and counting in a hemocytometer for a sample of scaffolds. Cell-loaded scaffolds were incubated and kept in DMEM/F12 medium with 10% fetal bovine serum for 24 hours before implanting into animals. Phenotype of the SCs was confirmed by immunochemical staining of positive S100 [13, 14, 40].

2.5. Animal experiments

All experiments involving animals were performed according to the guidelines approved by the Mayo Clinic Institutional Animal Care and Use Committee (IACUC). Animals were housed according to National Institutes of Health (NIH) and U. S. Department of Agriculture guidelines. All rats were held on a 12-hour light-dark cycle on a standard regimen, with food and water ad libitum in conventional housing. A total of 33 adult female Sprague-Dawley rats (Charles River Laboratories, Wilmington, Massachusetts; Harlan Laboratories, Indianapolis, Indiana) weighing between 200 to 250 grams were used. Female rats were used in this study because of the ease of handling bladder squeezing and the lessened incidence of urinary tract infection compared to males. Bladders were squeezed twice per day, and rats were given analgesics and antibiotics as needed after surgery. All rats were cared for with availability of veterinarians experienced in handling rodents with spinal cord injury in 24 hours [13].

2.6. Surgical procedures, spinal cord transection, and scaffold implantation

Before surgery, all animals were given 5 ml of lactated Ringer's solution (Baxter Healthcare Corporation, Deerfield, Illinois) subcutaneously, Buprenex (0.05 mg/kg, Reckitt Benckiser Pharmaceuticals Inc, Richmond, Virginia) intramuscularly, Baytril (65 mg/kg, Bayer Corporation, Shawnee, Kansas) intramuscularly, and had access to Acetaminophen (Mapap™ Major Pharmaceutiacals, Livonia MI) in their drinking water (1:15) for 24 hours previously [13].

Female rats were randomly designated to each of four experimental groups for the implantation of SC-loaded multi-channel scaffolds fabricated from PLGA, PCLF, OPF and OPF+. Laminectomy was carried out at $T_{9/10}$ level followed by complete transection of spinal cord and implantation of scaffold. Briefly, rats were anesthetized with intraperitoneal injection of ketamine at a concentration of 80 mg/kg (Fort Dodge Animal Health) and xylazine at a concentration of 5 mg/kg (Lloyd Laboratories, Shenandoah, Iowa). The back was shaved and aseptically prepared with a povidone-iodine scrub swabstick (Professional Disposables Inc, Orangeburg, New York). Puralube Vet Ointment (Pharmaderm, Melville, New York) was spread to prevent the eyes from dehydration during the long surgical procedures. Rats were maintained on heating pad to keep body temperature at 37°C ± 0.5°C during surgical procedures. A Zeiss F170 microsurgical microscope (Oberkochen, Germany) was used along with a sterile technique during the whole surgical procedures. Following skin incision and laminectomy at the T_9 or T_{10} vertebral level, spinal cord was completely cut by a sharp blade (No 11, BD Medical, Batavia, IL). A microhook/probe was used to confirm the completeness of transection between the 2 cut ends. After complete transection, the spinal cord retracted from the injury location and yielded a 2-mm break at T_9 or T_{10} level of spinal cord. All visible spinal roots were removed from the transection gap. A 2-mm long scaffold (PLGA, PCLF, OPF or OPF+) loaded with SCs was implanted into the gap by

a fine forceps and aligned with the rostral and caudal spinal cord stumps, making a tight contact with the both ends under the surgical scope. Muscles and skin were sutured separately in layers, with a deep and tight first suture of the muscle in order to hold and fix the implanted scaffold stable in the gap.

2.7. Postoperative care of animals

The animals were maintained in low-sided and warmed cages to allow them to easily reach food and water. Deep bedding was changed frequently in order to prevent decubitus ulcers. Buprenex (0.05 mg/kg; Reckitt Benckiser Pharmaceuticals Inc, Richmond, Virginia) was administered intramuscularly twice per day for 3 to 5 days to lessen pain after transection surgery. Acetaminophen was given in the drinking water for 1 day preoperatively and 7 days post operatively. Baytril (65 mg/kg; Bayer Corporation, Shawnee, Kansas) was given intramuscularly twice a day for the first week after surgery and as needed thereafter to prevent infection. Five mls of saline was also given twice a day for the first five days post surgery. Bladders were squeezed empty manually twice a day for the whole duration after transection, during which time the urine stream assessed for signs of infection.

2.8. Tissue preparation and sectioning

Rats were humanely euthanized by deep anesthesia with an intraperitoneal injection of 0.4 ml pentobarbital sodium (40 mg/kg) (Fort Dodge Animal Health, Fort Dodge, IA) and transcardially perfused with fixative (4% paraformaldehyde) 1 month after cord transection surgery. During the perfusion, 60 ml of PBS was infused through the aorta, followed by 60 ml of 4% paraformaldehyde. The spinal column and cord with the implants were removed *en bloc* and post-fixed overnight in the same fixative at 4° C. Following post-fixation, implanted scaffolds including 5 mm of the rostral and caudal spinal cord of the grafted area, were dissected free from the vertebral column, fixed again in the same fixative overnight at 4°C before they were processed for paraffin-embeddi ng. The spinal cord segments were cut transversely into 8-μm sections on a Reichert-Jung Biocut microtome (Leica, Bannockburn, IL). Sections were carefully numbered and sequentially collected as 5 sections per slide.

2.9. Neurofilament (NF) staining

NF staining and counting techniques were used to quantitatively assess the regenerated axons through the scaffold with 7-channels implanted after cord transection ($T_{9/10}$) [11]. Scaffold sections were selected at quarter length intervals from the rostral scaffold-cord interface, to the scaffold mid-point and to the caudal scaffold-cord interface. Sections were deparaffinized in xylene, rehydrated in graded ethanol and rinsed in distilled water. In order to retrieve the antigen, the sections were incubated in Proteinase K (2 μg/ml) diluted 1:10 with phosphate buffered saline (PBS) for 20 min at room temperature. Endogenous peroxidases were quenched by incubating sections in 0.3% hydrogen peroxidase in methanol for 30 minutes, rinsed in PBS for 5 min before they were covered with a protein block solution (InnoGenex, San Ramon, CA) for 20 min to suppress nonspecific binding of subsequent reagents. The sections were incubated with the biotinylated monoclonal mouse anti-NF antibody against phosphorylated NF-H (Dako clone 2F11, Carpinteria, CA), diluted 1:50 and incubated overnight at 4 °C. Goat anti-mouse secondary was conjugated to horseradish peroxidase with streptavidin, and the stain was visualized using hydrogen peroxide and the DAB chromogen (Envision system, Dako) [11].

2.10. Counting of NF-stained axons

The number of NF-stained axons was tallied at three levels along the scaffold as previously described [11]: 1/4 of the distance, 2/4 of the distance and 3/4 of the distance between the rostral and caudal scaffold-cord junctions. Axon profiles were readily identified in 8 μm

transverse sections of tissues. They appeared as small russet-colored cylinders when the observer focuses through the section (as in Figure 4). All axon tallies were done three times to get an average number of counting for each section by a blinded observer to reduce bias.

2.11. Analysis of scar and cyst formation

The volume of glial scarring and cyst formation at both rostral and caudal spinal cord-scaffold interfaces was measured as previously described [32, 41]. Selected slides at a 200μm interval from the scaffold within the above-mentioned interface area were deparaffinized and rehydrated as previously described. Sections were stained with hematoxylin (Thermo Fisher Scientific, Santa Clara, CA) and Gomori's trichrome stain solution (Sigma Aldrich). Following a wash in 1% acetic acid and distilled H_2O, sections were dehydrated in serially ascending concentrations of ethanol and then 5 changes of xylol. Slides were cover-slipped with a synthetic xylol-based mounting media. Image acquisition was carried out by using a Zeiss AxioCam set on a Zeiss Axio Imager Z1 microscope. Zeiss KS400 software was applied to measure the volume of normal cord, scar formation as well as cyst formation. The same measurements were used for all analyzed tissues. All of these analyses were performed by a blinded observer. Cyst was identified as fluid-filled cavity. Scarring was observed as spinal cord tissue that was infiltrated with collagen because collagen is not found in normal spinal cord.

2.12. Behavioral evaluation

Behavioral analysis was performed at the same time by three observers blinded to the treatments at week 2 and week 4, respectively, using a battery of tests to rate open-field locomotion by the Basso–Beattie–Bresnahan (BBB) scale [42].

2.13. Statistical analysis

The numbers of NF-stained axons, BBB scores and the volumes of scar and cyst were described by mean and SEM. Difference in number of these parameters between groups was analyzed with one-way analysis of variance (ANOVA). The statistical significance of difference ($P < 0.05$) in parameters was determined by parametric one-way ANOVA.

Results

3.1. Mechanical property of polymer scaffolds

Compression and flexural moduli of conduits are shown in Fig 1. As shown in Fig. 1A, PLGA had the highest flexural modulus (66.33±7.01 MPa) as compared to the other polymer groups and fresh spinal cord (0.74±0.14 MPa). There was no significant difference in 3-point bending between fresh spinal cord and OPF+ or OPF polymer ($P > 0.05$). There was a significant difference in 3-point bending between fresh spinal cord and PCLF and PLGA polymers ($P < 0.0001$). Interestingly, a significant difference in the 3-point bending test was found between PLGA and PCLF, PLGA and OPF, PLGA and OPF+, PCLF and OPF, PCLF and OPF+ ($P < 0.0001$) (Fig 1A). No significant difference in compression modulus was identified between fresh spinal cord and OPF+, OPF and PLGA polymers ($P > 0.05$) (Fig. 2B). PCLF polymer had a significantly higher compression modulus compared to spinal cord and the other three polymers ($P < 0.0001$) (Fig 1B)

3.2. Macroscopic morphology and alignment of polymer scaffolds in spinal cords

Geometrical and dimensional properties of the scaffolds were reproducible and were maintained during cell-loading and neurosurgical implantation. All types of scaffolds possessed macro-architecture consistent with original mold design (Fig 2A, 2B, 2C and 2D). Gross examination of excised segments of spinal cord and implant revealed that all the

scaffolds were well positioned between the rostral and caudal stumps with good alignment. The implants integrated fully with the host tissue without apparent cavity or gap between the implanted scaffold and host (Fig 2E, 2F, 2G and 2H). The dorsal surface of the spinal cord showed a grossly normal appearance immediately adjacent to the reconstructed segments, with no evidence of atrophy of the spinal stumps. Among all cases, a high degree of integration between scaffolds and the host tissues was achieved, although OPF+, OPF and PCLF showed better alignment than PLGA polymer. As a result, the reconstructed spinal cord segments exhibited a macroscopic appearance**,** which was comparable to intact spinal cord. Moreover, OPF+, OPF and PCLF scaffolds better retained their original shape than PLGA (Fig 2). This was consistent with previous observations showing that PLGA scaffolds may become misaligned [43].

3.3. Axonal growth

NF-immunolabeling showed that axons grew into the implants in the all polymer scaffolds seeded with SCs (Fig 3). Axons were identified as immuno-stained, russet-colored cylinders that could be clearly visualized as tubular when the observer focused through the section under the microscope. Representative sections from each polymer type at lower magnification (Fig 3A, 3B, 3C and 3D), and higher magnification (Fig 3E, 3F, 3G and 3H) are shown.

3.4. Axonal orientation and distribution

Two different growth patterns of axonal regeneration were seen within the channels of scaffolds. Within the body of the scaffold most axons were oriented in parallel to the longitudinal axis of the channel and thus appeared as discrete pinpoints of NF staining (Fig 4A). At the ends of the scaffolds axons appeared to be growing at more random angles to the channel axis (Fig 4B). This latter pattern was found most commonly at the caudal interface, suggesting that axonal orientation may have changed upon encountering scarring.

We also found that the NF-stained axons were either concentrated within the center of the scaffold channels or dispersed in the peripheral parts of the scaffold channels, depending on the polymer used. In OPF+ scaffolds, axons were densely centered in the channel core that was clearly demarcated from circumferential, laminar tissue (Fig 4C). In the other polymer groups (PLGA, PCLF and OPF) a more scattered distribution of regenerating axons was observed (Fig 4D). The distribution differed with different polymer types. The percentages of channels with a centralized pattern in each polymer group was for PLGA 4.75 ± 2.7%, for PCLF 9.46 ± 3.7%, for OPF 37.09 ± 6% and for OPF+ 85.50 ± 4.3% (Fig 4E). These differences were highly significant ($P < 0.0001$) in percentages between OPF+ and PLGA ($P < 0.0001$), OPF and PLGA ($P < 0.0001$), OPF+ and PCLF ($P < 0.0001$), OPF+ and OPF ($P < 0.0001$), OPF+ and OPF ($P < 0.0001$) polymer groups. No significant difference was identified between PLGA and PCLF polymer groups. Furthermore, a relationship existed between the distribution pattern of axons and the number of regenerated axons per channel per animal. A significantly higher number of regenerated axons was associated with the centralized pattern compared to the dispersed pattern ($P < 0.05$) (Fig 4F).

3.5. Axonal count

NF staining was used to quantify axonal regeneration in each of the SC-loaded polymer groups. Axons were found within distinct channels and also within pores of the biodegradable scaffolds. The average number of axons per channel of the scaffold in transverse sections selected from one quarter (1/4), one half (2/4), and three quarters (3/4) levels through the scaffold for each animal was analyzed in this study. All of the polymers supported axonal growth. OPF+, OPF and PCLF implants seeded with SCs showed more axons than the implants of PLGA with SCs (Fig 5). OPF+ supported the highest number of

regenerating axons. ANOVA analysis showed that significantly higher axon counting was found in PCLF ($P < 0.01$) and OPF+ ($P < 0.05$) groups, compared to that of PLGA group. Neutral OPF scaffolds transplanted with SCs also contained more axons than the PLGA polymer implants although no statistically significant difference was demonstrated ($P > 0.05$) (Fig 5).

3.6. Glial Scar and cyst cavity formation

Image analysis of Gomori trichrome stained sections was used to identify the volumes of scar tissue at the rostral and caudal spinal cord interfaces between the implanted scaffolds. Volume of scar and cyst rostral and caudal to the implanted scaffold was measured and a comparison was made between the polymer groups. No significant difference was found in the scar volumes (both rostral and caudal) between the groups studied (Fig 6A) except for a significantly smaller cyst volume in both the rostral and caudal interfaces in the PLGA group, compared to PCLF group ($P < 0.05$) (Fig 6B). However, there were no differences when both the scar and cyst volumes were combined together as a whole (Fig 6C).

3.7. Functional analysis/BBB Scores

Recovery of locomotor function was evaluated using the BBB rating scale [42]. Although there were significant differences in the axonal counts in the groups described above, no significant differences in BBB motor function testing were observed between animals in the four different polymer groups after 2 and 4 weeks following scaffold implantation. Furthermore there were no overall functional improvements noted over the course of the experiment. The BBB scores for the 2 week time-point were 4.621 ± 0.9181, 5.518 ± 0.7054, 5.833 ± 0.9717 and 3.761 ± 0.928 for the PLGA, PCLF, OPF and OPF+ polymers, respectively. The 4 week time-point scores were 4.524 ± 1.066, 4.037 ± 0.8195, 5.400 ± 0.6528 and 4.144 ± 0.8508 for the PLGA, PCLF, OPF and OPF+ polymers, respectively (Fig 7).

Discussion

Axonal regeneration is fundamental for spinal cord repair and functional recovery after spinal cord injury [13, 44–46]. The aim of this study was to use a model system to quantitatively compare the regenerative capacity of four polymer types as implants within a spinal cord transection model. Schwann cells have been consistently shown to be one of the most effective therapeutic cell types in transplantation and regeneration after experimental spinal cord injury [23–26, 47–50]. These cells reduce the size of spinal cysts, remyelinate axons [13] and improve functional recovery in spinal cord injury [51–53]. They have also been shown to produce a number of growth factors that initiate and support the growth of axons, and that these cells express cell adhesion molecules on their surface for axon guidance [54]. The polymers used here included PLGA [10, 11, 13, 14, 17], PCLF [34, 55], OPF and OPF+ [12, 56]. We have shown improved regeneration capacity with schwann cell-seeded PLGA scaffolds over scaffolds seeded with neuronal stem cells [14]. With regards to OPF and schwann cell viability, tissue culture data also showed that the positively charged hydrogel polymer supported both neuronal outgrowth from dorsal root ganglia explants, improved schwann cell attachments and migration and contributed to neurite myelination [12]. In the present study, significantly higher axonal counts were seen in PCLF and OPF+ groups compared to the PLGA groups as a control. PLGA scaffolds have been extensively studied by our research group [11, 13, 14, 17] and were thus used as the benchmark to compare novel polymers such as fumarate composites. The present study is the first to demonstrate the enhanced capacity of OPF+ to support axonal regeneration *in vivo* when combined with schwann cell delivery.

A variety of biomaterials have been used for implantation into the injured cord in an attempt to recover neurologic function [57–60]. However, few studies have shown a high degree of polymer integration with the surrounding tissue [61–64]. The major difficulties were the filling and holding of the injected cells in the lesion cavities [65]. These cavities or cysts became an important physical obstacle for axonal regeneration, structural rebuilding and functional recovery. Compared to PLGA, OPF, OPF+ and PCLF conduits showed better interaction with the surrounding host tissue, filling the gap and building a bridge across which axons were able to grow into the implants. They also exhibited smoother integration into the host tissue, although we were not able to demonstrate a significant difference in scar volumes compared to the PLGA group. To improve the integration of the implants, we have been developing and modifying our surgical techniques to minimize the injury/trauma induced by the transection/implant on the rat transection model. Such modifications have included making smaller laminectomies, minimizing the incision through dura, implementing quick and complete transection of the cord, rigid fixation and ensuring there is a gap between spinal cord ends that accurately accommodates the scaffold size. Other techniques have included minimizing bleeding, suturing the muscle tightly in order to hold and fix the implanted scaffold in good alignment with the rostral and caudal stumps [43].

Rapid progress in study of hydrogel chemistry has produced the materials more suitable for the spinal cord in respect to their mechanical properties. Highly hydrated and soft polymers have similar properties to spinal cord tissue [10]. Our results show that PLGA and PCLF have higher flexural modulus compared to OPF and OPF+, indicating that they are more resistant to bending. However, at the same loading condition, PCLF has a compression modulus of 8.4 MPa, which is about 20 times higher than PLGA and 44 times higher than fresh spinal cord. OPF and OPF+ contain a large amount of water that decreases both flexural and compression modulus of these materials similar to fresh spinal cord tissue with high porosity and large water content. In our experience, OPF polymers, charged and non-charged, possess the best texture or physical properties compatible with normal spinal cord tissues. PLGA is relatively rigid compared to the soft OPF and OPF+ hydrogels, while PCLF has more flexibility in bending as compared to PLGA. Among the four polymers in the present study, PCLF showed significantly higher compression modulus than other three polymers (PLGA, OPF and OPF+) as well as the fresh spinal cord. This may explain why the volume of cyst in the PCLF polymer group was significantly higher than the volume of cyst in PLGA scaffolds. PCLF scaffolds may lead to more compressive damage of the blood vessels and leave bigger volumes of cyst in the injured area of the transected cord.

Hydrogel scaffolds also have advantages in spinal cord regeneration with a three-dimensional porous structure, their chemical and physical properties, and their diffusion parameters. Biocompatibility also extends to the degree of inflammation the material may cause *in vivo*. We have previously investigated the biocompatibility and biodegradation of both OPF and OPF+ in a rat cage model [9] and did not observe any increased inflammatory response compared to empty cage and PLGA control groups (unpublished data). These materials can therefore provide a scaffold for ingrowth of neural tissue that will subsequently degrade after regeneration. Gradients and surface charge modification for cell adhesion can also be constructed on functionalized synthetic polymers [10]. The influence of surface charge on cell growth has been investigated and it is now well known that many types of cells adhere better to positively charged surface [66]. OPF+ polymers may have a better attachment attribute *in vivo* so the implanted growth-promoting cells attach to the channel walls. This may facilitate the newly regenerated axons infiltrating into the central part of the channels by providing a contact guidance for the axonal regeneration and allow nerve fibers to extend across the entire channels of the scaffold. In the present study, highest percentage of the centralized infiltrating axons in the channels happened in the OPF+ polymer groups. Moreover, polymers with the centralized pattern showed significant higher

number of regenerated axons compared to the dispersed pattern. Another recent study using an *in vivo* hemisection model of spinal cord injury assessed the ingrowth of neuronal tissue elements in hydrogels with different charges. Neurofilaments were similarly demonstrated to infiltrate the central part of the hydrogels most plentifully in the copolymers with positive charges [67].

In a previous study we developed a synthetic, positively charged hydrogel as a substrate for nerve cell attachment and neurite outgrowth in cultures. Positively charged OPF improved primary sensory rat neuron attachment and differentiation dose-dependently. Positively charged hydrogels also helped to support attachment of dorsal root ganglion (DRG) explants that contain sensory neurons and SCs. Taken together all these findings indicate that charged OPF hydrogels are able to sustain both primary nerve cells and neural supporting cells that are important for neural regeneration [12]. Others studied the injury and repair of transected sciatic nerves in adult mice by charged guidance channels [68]. Significantly more myelinated axons has been found in the nerves that regenerated in positively charged channels compared to those in uncharged channels. Although the mechanism for the biological effects of the positive electrical charge is not clear, a defined calcium concentration may be important for optimal neurite outgrowth [69]. These data indicate that the existence of positive charge on a cell attachment surface is a critical factor in the subsequent behaviors of the cells that anchor on the surfaces. The positively charged OPF hydrogels used in the present study represent a group of promising candidate scaffolds for neural tissue engineering applications.

Spinal cord injury results in the formation of scars and cysts. In the acute phase of spinal cord injury, hemorrhage occurs around the injured sites, leading to a disruption in oxygen and nutrient supply to all cells and tissues in the injured area. The fluid-filled cysts caused by the inflammatory response together with the vascular damage owing to the spinal cord injury can thereafter form and expand progressively at the injured site, and subsequently contribute to cell death and inhibition of axonal regeneration [70, 71]. Glial scar formation occurs usually in the second phase of spinal cord injury. This scar has been well demonstrated as another major inhibitory barrier to axonal regeneration after spinal cord injury [70, 72, 73]. Biomaterial scaffolds with salt-leached porous poly (epsilon-caprolactone) have been designed to compare different channel architecture and the influence that the overall design may have in spinal cord transection. Wong and colleagues [74] demonstrated that open-path designs permitted larger penetration of GFAP-labeled neural tissues from both stumps and resulted in less scarring than the conventional implant designs (no open-path designs). The open-path design, which is very similar to our scaffolds, provided contact guidance and allowed nerve axons to extend across the entire length of the implanted scaffolds [74]. Scaffolds with optimal designs may impede scarring and subsequent cyst formation. PLGA scaffolds have been demonstrated to prevent scarring and cyst formation in the animal models of SCI [63, 75]. In this study we also found a smaller volume of cyst in PLGA polymer group than the PCLF polymer group. This would be compatible with our previous observation that minimizing vascular damage reduces cyst formation [76]. Thus scaffolds with mechanical properties most closely resembling the host tissue produce better outcomes.

The scaffold could serve as a bridge to facilitate to guide the regenerating axons across the injury site and to recover connections with the target of innervation to support functional recovery [54]. Functional recovery was not seen in any of the animal groups at both 2 and 4 weeks, as assessed by the BBB locomotor scale. We hypothesized that a certain threshold number of regenerated axon numbers would be required to exert a significant and detectable functional recovery after the injury in this time frame. Clearly, not all the counted axons reach and connect to target neurons correctly and functionally, and indeed we observed

variablility in the direction of axonal growth that was dependent upon the polymer type. It is also probable that a four week time frame is insuffient to observe functional recovery following complete transection. It is unlikely that regenerated axons have been able to arrive at the correct destination and estalish functional connections. We recently demonstrated by axon tracing studies that regenerated axons through schwann cell loaded PLGA scaffold extended for up to 15 mm beyond the scaffold into the distal cord. However, even after 2 months functional improvement was not observed [13]. Nevertheless, the negative results in functional assssment are also consistent with our previous studies [14]. Future studies will be designed to explore approaches to enhance connectivity using optimized scaffolds for time-released delivery of therapeutic agents.

Conclusions

Our study directly compared four polymer scaffold types each loaded with schwann cells. All of the studied polymers (PLGA, PCLF, OPF and OPF+) supported axonal growth from the injured spinal cord neurons. OPF+ and PCLF had excellent capacity for supporting regeneration of axons into the scaffolds. OPF+ polymer uniquely exhibited axonal regeneration with centralized pattern that resulted in a concentrated number of regenerated axons in the channels of scaffolds. Overall this pattern was strongly associated with increased numbers of regenerated axons regardless of the polymer type. Since this pattern was most commonly seen with OPF+, this polymer may represent a good choice of material with which to further study spinal cord repair. We are optimizing conditions for axonal growth in the spinal cord in terms of cells and external cell milieu factors. A much longer period of observation will be required to study functional improvement in spinal cord injury animals in future study. Our data may provide a basis for future strategies toward spinal cord repair in patients. The model will provide a quantitative basis for evaluating individual and combined therapeutic strategies.

Acknowledgments

This work was supported by a grant from the NIH (EB002390) and the Kipnis, Morton, Wilson, and Mayo Foundations (AJW).

We thank James Tarara for his critical help in imaging of the axon counting and measure of the scar and cyst formation. We thank Jane Meyer for her administrative role in manuscript preparation. This work was supported by a grant from the NIH (EB02390) and the Wilson, Morton, Neilsen and Mayo Foundations (AJW).

References

1. McDonald JW, Sadowsky C. Spinal-cord injury. Lancet. 2002; 359(9304):417–425. [PubMed: 11844532]
2. Schwab ME. Repairing the injured spinal cord. Science. 2002; 295:1029–1031. [PubMed: 11834824]
3. Pachence, JM.; Kohn, J. Biodegradable polymers for tissue engineering. In: Lanza, RP.; Langer, R.; Chick, WL., editors. Principles of Tissue Engineering. Austin: R.G. Landes and Company; 1997. p. 273-293.
4. Patrick, CW.; Mikos, AG.; McIntire, LV. Frontiers in Tissue Engineering. Oxford Pergamon Press; 1998.
5. Bareyre FM. Neuronal repair and replacement in spinal cord injury. J Neurol Sci. 2008; 265(1–2): 63–72. [PubMed: 17568612]
6. Shoichet, MS.; Hubbel, JA. Polymers for Tissue Engineering. Utrecht: VSP; 1998.
7. Blacher S, Maquet V, Schils F, Martin D, Schoenen J, Moonen G, et al. Image analysis of the axonal ingrowth into poly(D,L-lactide) porous scaffolds in relation to the 3-D porous structure. Biomaterials. 2003; 24(6):1033–1040. [PubMed: 12504525]

8. Runge MB, Dadsetan M, Baltrusaitis J, Knight AM, Ruesink T, Lazcano EA, et al. The development of electrically conductive polycaprolactone fumarate-polypyrrole composite materials for nerve regeneration. Biomaterials. 2010; 31(23):5916–5926. [PubMed: 20483452]
9. Kim J, Dadsetan M, Ameenuddin S, Windebank AJ, Yaszemski MJ, Lu L. In vivo biodegradation and biocompatibility of PEG/sebacic acid-based hydrogels using a cage implant system. J Biomed Mater Res A. 2010; 95(1):191–197. [PubMed: 20574982]
10. Madigan NN, McMahon S, O'Brien T, Yaszemski MJ, Windebank AJ. Current tissue engineering and novel therapeutic approaches to axonal regeneration following spinal cord injury using polymer scaffolds. Respir Physiol Neurobiol. 2009; 169:183–199. [PubMed: 19737633]
11. Krych AJ, Rooney GE, Chen B, Schermerhorn TC, Ameenuddin S, Gross L, et al. Relationship between scaffold channel diameter and number of regenerating axons in the transected rat spinal cord. Acta Biomater. 2009; 5(7):2551–2559. [PubMed: 19409869]
12. Dadsetan M, Knight AM, Lu L, Windebank AJ, Yaszemski MJ. Stimulation of neurite outgrowth using positively charged hydrogels. Biomaterials. 2009; 30(23–24):3874–3881. [PubMed: 19427689]
13. Chen BK, Knight AM, de Ruiter GCW, Yaszemski MJ, Currier BL, Windebank AJ. Axon regeneration through scaffold into distal spinal cord after transection. J Neurotrauma. 2009; 26(10):1759–1771. [PubMed: 19413501]
14. Olson HE, Rooney GE, Gross L, Nesbitt JJ, Galvin KE, Knight A, et al. Neural stem cell- and schwann cell-loaded biodegradable polymer scaffolds support axonal regeneration in the transected spinal cord. Tissue Eng Part A. 2009; 15(7):1797–1805. [PubMed: 19191513]
15. de Ruiter GC, Onyeneho IA, Liang ET, Moore MJ, Knight AM, Malessy MJ, et al. Methods for in vitro characterization of multichannel nerve tubes. J Biomed Mater Res A. 2008; 84(3):643–651. [PubMed: 17635012]
16. Jabbari E, Wang S, Lu L, Gruetzmacher JA, Ameenuddin S, Hefferan TE, et al. Synthesis, material properties, and biocompatibility of a novel self-cross-linkable poly(caprolactone fumarate) as an injectable tissue engineering scaffold. Biomacromolecules. 2005; 6(5):2503–2511. [PubMed: 16153086]
17. Moore MJ, Friedman JA, Lewellyn EB, Mantila SM, Krych AJ, Ameenuddin S, et al. Multiple-channel scaffolds to promote spinal cord axon regeneration. Biomaterials. 2006; 27(3):419–429. [PubMed: 16137759]
18. Honma H, Podratz JL, Windebank AJ. Acute glucose deprivation leads to apoptosis in a cell model of acute diabetic neuropathy. J Periph Nerv Syst. 2003; 8:65–74.
19. Zhu X, Lu L, Currier BL, Windebank AJ, Yaszemski MJ. Controlled release of NFκB decoy oligonucleotides from biodegradable polymer microparticles. Biomaterials. 2002; 23:2683–2692. [PubMed: 12059017]
20. Gill JS, Zhu X, Moore MJ, Lu L, Yaszemski MJ, Windebank AJ. Effects of NFκB decoy oligonucleotides released from biodegradable polymer microparticles on a glioblastoma cell line. Biomaterials. 2002; 23:2773–2781. [PubMed: 12059028]
21. Friedman JA, Windebank AJ, Moore MJ, Spinner RJ, Currier BL, Yaszemski MJ. Biodegradable polymer grafts for surgical repair of the injured spinal cord. Neurosurgery. 2002; 51:742–752. [PubMed: 12188954]
22. Podratz JL, Rodriguez EH, DiNonno ES, Windebank AJ. Myelination by Schwann cells in the absence of extracellular matrix assembly. Glia. 1998; 23:383–388. [PubMed: 9671968]
23. Pinzon A, Calancie B, Oudega M, Noga BR. Conduction of impulses by axons regenerated in a Schwann cell graft in the transected adult rat thoracic spinal cord. J Neurosci Res. 2001; 64:533–541. [PubMed: 11391708]
24. Oudega M, Gautier SE, Chapon P, Fragoso M, Bates ML, Parel JM, et al. Axonal regeneration into Schwann cell grafts within resorbable poly(α-hydroxyacid) guidance channels in the adult rat spinal cord. Biomaterials. 2001; 22:1125–1136. [PubMed: 11352092]
25. Xu XM, Zhang SX, Li H, Aebischer P, Bunge MB. Regrowth of axons into the distal spinal cord through a Schwann-cell-seeded mini-channel implanted into hemisected adult rat spinal cord. Eur J Neurosci. 1999; 11:1723–1740. [PubMed: 10215926]

26. Bunge MB. Bridging the transected or contused adult rat spinal cord with Schwann cell and olfactory ensheathing glia transplants. Prog Brain Res. 2002; 137:275–282. [PubMed: 12440373]
27. Dadsetan M, Szatkowski JP, Yaszemski MJ, Lu L. Characterization of photo-cross-linked oligo[poly(ethylene glycol) fumarate] hydrogels for cartilage tissue engineering. Biomacromolecules. 2007; 8(5):1702–1709. [PubMed: 17419584]
28. Dadsetan M, Liu Z, Pumberger M, Giraldo CV, Ruesink T, Lu L, et al. A stimuli-responsive hydrogel for doxorubicin delivery. Biomaterials. 2010; 31(31):8051–8062. [PubMed: 20696470]
29. Shin H, Quinten Ruhe P, Mikos AG, Jansen JA. In vivo bone and soft tissue response to injectable, biodegradable oligo(poly(ethylene glycol) fumarate) hydrogels. Biomaterials. 2003; 24(19):3201–3211. [PubMed: 12763447]
30. Temenoff JS, Athanasiou KA, LeBaron RG, Mikos AG. Effect of poly(ethylene glycol) molecular weight on tensile and swelling properties of oligo(poly(ethylene glycol) fumarate) hydrogels for cartilage tissue engineering. J Biomed Mater Res. 2002; 59(3):429–437. [PubMed: 11774300]
31. Holland TA, Tabata Y, Mikos AG. Dual growth factor delivery from degradable oligo(poly(ethylene glycol) fumarate) hydrogel scaffolds for cartilage tissue engineering. J Control Release. 2005; 101(1–3):111–125. [PubMed: 15588898]
32. Rooney GE, Knight AM, Madigan NN, Gross L, Chen B, Giraldo CV, et al. Sustained delivery of dibutyryl cyclic adenosine monophosphate to the transected spinal cord via oligo [(polyethylene glycol) fumarate] hydrogels. Tissue Eng Part A. 2011; 17(9–10):1287–1302. [PubMed: 21198413]
33. Tsai EC, Dalton PD, Shoichet MS, Tator CH. Synthetic hydrogel guidance channels facilitate regeneration of adult rat brainstem motor axons after complete spinal cord transection. J Neurotrauma. 2004; 21(6):789–804. [PubMed: 15253805]
34. Wang S, Yaszemski MJ, Knight AM, Gruetzmacher JA, Windebank AJ, Lu L. Photo-crosslinked poly(ε-caprolactone fumarate) networks for guided peripheral nerve regeneration: Material properties and preliminary biological evaluations. Acta Biomater. 2009; 5(5):1531–1542. [PubMed: 19171506]
35. Behravesh E, Sikavitsas VI, Mikos AG. Quantification of ligand surface concentration of bulk-modified biomimetic hydrogels. Biomaterials. 2003; 24(24):4365–4374. [PubMed: 12922149]
36. Brockes JP, Fields KL, Raff MC. Studies on cultured rat Schwann cells. I. Establishment of purified populations from cultures of peripheral nerve. Brain Research. 1979; 165:105–118. [PubMed: 371755]
37. Porter S, Clark MB, Glaser L, Bunge RP. Schwann cells stimulated to proliferate in the absence of neurons retain full functional capability. Journal of Neuroscience. 1986; 6:3070–3078. [PubMed: 3760949]
38. Xu XM, Guenard V, Kleitman N, Bunge MB. Axonal regeneration into Schwann cell-seeded guidance channels grafted into transected adult rat spinal cord. J Comp Neurol. 1995; 351:145–160. [PubMed: 7896937]
39. Guenard V, Kleitman N, Morrissey TK, Bunge RP, Aebischer P. Syngeneic Schwann cells derived from adult nerves seeded in semipermeable guidance channels enhance peripheral nerve regeneration. J Neurosci. 1992; 12(9):3310–3320. [PubMed: 1527582]
40. Morrissey TK, Kleitman N, Bunge RP. Isolation and functional characterization of Schwann cells derived from adult peripheral nerve. Journal of Neuroscience. 1991; 11:2433–2442. [PubMed: 1869923]
41. Rodriguez FJ, Verdu E, Ceballos D, Navarro X. Nerve guides seeded with autologous schwann cells improve nerve regeneration. Exp Neurol. 2000; 161(2):571–584. [PubMed: 10686077]
42. Basso DM, Beattie MS, Bresnahan JC. A sensitive and reliable locomotor rating scale for open field testing in rats. J Neurotrauma. 1995; 12:1–21. [PubMed: 7783230]
43. Rooney GE, Vaishya S, Ameenuddin S, Currier BL, Schiefer TK, Knight A, et al. Rigid fixation of the spinal column improves scaffold alignment and prevents scoliosis in the transected rat spinal cord. Spine. 2008; 33(24):E914–919. [PubMed: 19011531]
44. Enomoto M, Wakabayashi Y, Qi ML, Shinomiya K. Present situation and future aspects of spinal cord regeneration. J Orthop Sci. 2004; 9(1):108–112. [PubMed: 14767714]
45. Gordon T, Sulaiman O, Boyd JG. Experimental strategies to promote functional recovery after peripheral nerve injuries. J Peripher Nerv Syst. 2003; 8(4):236–250. [PubMed: 14641648]

46. Hase T, Kawaguchi S, Hayashi H, Nishio T, Mizoguchi A, Nakamura T. Spinal cord repair in neonatal rats: a correlation between axonal regeneration and functional recovery. Eur J Neurosci. 2002; 15(6):969–974. [PubMed: 11918656]

47. Takami T, Oudega M, Bates ML, Wood PM, Kleitman N, Bunge MB. Schwann cell but not olfactory ensheathing glia transplants improve hindlimb locomotor performance in the moderately contused adult rat thoracic spinal cord. J Neurosci. 2002; 22:6670–6681. [PubMed: 12151546]

48. Pearse DD, Pereira FC, Marcillo AE, Bates ML, Berrocal YA, Filbin MT, et al. cAMP and Schwann cells promote axonal growth and functional recovery after spinal cord injury. Nat Med. 2004; 10(6):610–616. [PubMed: 15156204]

49. Novikova LN, Pettersson J, Brohlin M, Wiberg M, Novikov LN. Biodegradable poly-beta-hydroxybutyrate scaffold seeded with Schwann cells to promote spinal cord repair. Biomaterials. 2008; 29(9):1198–1206. [PubMed: 18083223]

50. Hurtado A, Moon LD, Maquet V, Blits B, Jerome R, Oudega M. Poly (D,L-lactic acid) macroporous guidance scaffolds seeded with Schwann cells genetically modified to secrete a bi-functional neurotrophin implanted in the completely transected adult rat thoracic spinal cord. Biomaterials. 2006; 27(3):430–442. [PubMed: 16102815]

51. Biernaskie J, Sparling JS, Liu J, Shannon CP, Plemel JR, Xie Y, et al. Skin-derived precursors generate myelinating Schwann cells that promote remyelination and functional recovery after contusion spinal cord injury. J Neurosci. 2007; 27(36):9545–9559. [PubMed: 17804616]

52. Lavdas AA, Chen J, Papastefanaki F, Chen S, Schachner M, Matsas R, et al. Schwann cells engineered to express the cell adhesion molecule L1 accelerate myelination and motor recovery after spinal cord injury. Exp Neurol. 2010; 221(1):206–216. [PubMed: 19909742]

53. Papastefanaki F, Chen J, Lavdas AA, Thomaidou D, Schachner M, Matsas R. Grafts of Schwann cells engineered to express PSA-NCAM promote functional recovery after spinal cord injury. Brain. 2007; 130(Pt 8):2159–2174. [PubMed: 17626035]

54. Tabesh H, Amoabediny G, Nik NS, Heydari M, Yosefifard M, Siadat SO, et al. The role of biodegradable engineered scaffolds seeded with Schwann cells for spinal cord regeneration. Neurochem Int. 2009; 54(2):73–83. [PubMed: 19084565]

55. Wang S, Kempen DH, Simha NK, Lewis JL, Windebank AJ, Yaszemski MJ, et al. Photo-Cross-Linked Hybrid Polymer Networks Consisting of Poly(propylene fumarate) and Poly(caprolactone fumarate): Controlled Physical Properties and Regulated Bone and Nerve Cell Responses. Biomacromolecules. 2008; (4):1229–1241. [PubMed: 18307311]

56. Hejcl A, Lesny P, Pradny M, Michalek J, Jendelova P, Stulik J, et al. Biocompatible hydrogels in spinal cord injury repair. Physiol Res. 2008; 57 (Suppl 3):S121–132. [PubMed: 18481908]

57. Dusart I, Schwab ME. Secondary cell death and the inflammatory reaction after dorsal hemisection of the rat spinal cord. Eur J Neurosci. 1994; 6(5):712–724. [PubMed: 8075816]

58. Schmidt CE, Leach JB. Neural tissue engineering: strategies for repair and regeneration. Annu Rev Biomed Eng. 2003; 5:293–347. [PubMed: 14527315]

59. Geller HM, Fawcett JW. Building a bridge: engineering spinal cord repair. Exp Neurol. 2002; 174(2):125–136. [PubMed: 11922655]

60. Bunge MB, Pearse DD. Transplantation strategies to promote repair of the injured spinal cord. J Rehabil Res Dev. 2003; 40(4 Suppl 1):55–62. [PubMed: 15077649]

61. Stokols S, Tuszynski MH. Freeze-dried agarose scaffolds with uniaxial channels stimulate and guide linear axonal growth following spinal cord injury. Biomaterials. 2006; 27(3):443–451. [PubMed: 16099032]

62. Prang P, Muller R, Eljaouhari A, Heckmann K, Kunz W, Weber T, et al. The promotion of oriented axonal regrowth in the injured spinal cord by alginate-based anisotropic capillary hydrogels. Biomaterials. 2006; 27(19):3560–3569. [PubMed: 16500703]

63. Teng YD, Lavik EB, Qu X, Park KI, Ourednik J, Zurakowski D, et al. Functional recovery following traumatic spinal cord injury mediated by a unique polymer scaffold seeded with neural stem cells. Proc Natl Acad Sci USA. 2002; 99:3024–3029. [PubMed: 11867737]

64. Patist CM, Mulder MB, Gautier SE, Maquet V, Jerome R, Oudega M. Freeze-dried poly(D,L-lactic acid) macroporous guidance scaffolds impregnated with brain-derived neurotrophic factor in the

transected adult rat thoracic spinal cord. Biomaterials. 2004; 25(9):1569–1582. [PubMed: 14697859]

65. Vroemen M, Aigner L, Winkler J, Weidner N. Adult neural progenitor cell grafts survive after acute spinal cord injury and integrate along axonal pathways. Eur J Neurosci. 2003; 18(4):743–751. [PubMed: 12925000]
66. Soekarno A, Lom B, Hockberger PE. Pathfinding by neuroblastoma cells in culture is directed by preferential adhesion to positively charged surfaces. Neuroimage. 1993; 1(2):129–144. [PubMed: 9343564]
67. Lesny P, Pradny M, Jendelova P, Michalek J, Vacik J, Sykova E. Macroporous hydrogels based on 2-hydroxyethyl methacrylate. Part 4: growth of rat bone marrow stromal cells in three-dimensional hydrogels with positive and negative surface charges and in polyelectrolyte complexes. J Mater Sci Mater Med. 2006; 17(9):829–833. [PubMed: 16932865]
68. Valentini RF, Sabatini AM, Dario P, Aebischer P. Polymer electret guidance channels enhance peripheral nerve regeneration in mice. Brain Res. 1989; 480(1–2):300–304. [PubMed: 2713656]
69. Kater SB, Mills LR. Regulation of growth cone behavior by calcium. J Neurosci. 1991; 11(4):891–899. [PubMed: 2010811]
70. Hagg T, Oudega M. Degenerative and spontaneous regenerative processes after spinal cord injury. J Neurotrauma. 2006; 23(3–4):264–280. [PubMed: 16629615]
71. Hulsebosch CE. Recent advances in pathophysiology and treatment of spinal cord injury. Adv Physiol Educ. 2002; 26(1–4):238–255. [PubMed: 12443996]
72. Yiu G, He Z. Glial inhibition of CNS axon regeneration. Nat Rev Neurosci. 2006; 7(8):617–627. [PubMed: 16858390]
73. Thuret S, Moon LD, Gage FH. Therapeutic interventions after spinal cord injury. Nat Rev Neurosci. 2006; 7(8):628–643. [PubMed: 16858391]
74. Wong DY, Leveque JC, Brumblay H, Krebsbach PH, Hollister SJ, Lamarca F. Macro-architectures in spinal cord scaffold implants influence regeneration. J Neurotrauma. 2008; 25(8):1027–1037. [PubMed: 18721107]
75. Lee SY, Oh JH, Kim JC, Kim YH, Kim SH, Choi JW. In vivo conjunctival reconstruction using modified PLGA grafts for decreased scar formation and contraction. Biomaterials. 2003; 24(27):5049–5059. [PubMed: 14559019]
76. Rooney GE, Endo T, Ameenuddin S, Chen B, Vaishya S, Gross L, et al. Importance of the vasculature in cyst formation after spinal cord injury. J Neurosurg Spine. 2009; 11(4):432–437. [PubMed: 19929340]

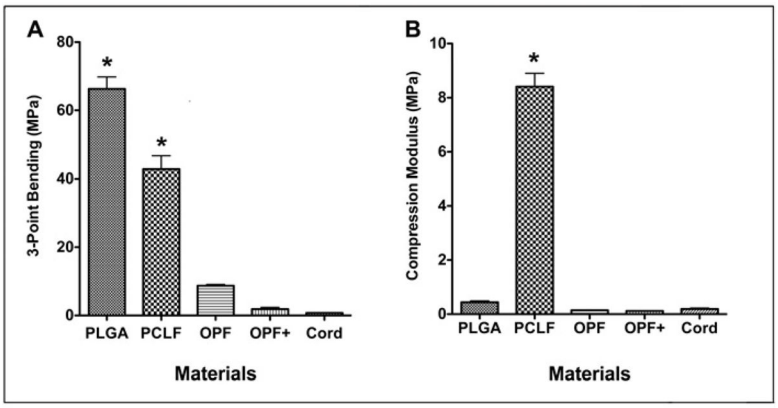

Figure 1.

Mechanical property of polymers and fresh spinal cord. (**A**) 3-point bending test; (**B**) Compression modulus test. *Significantly different as compared to spinal cord ($P < 0.0001$).

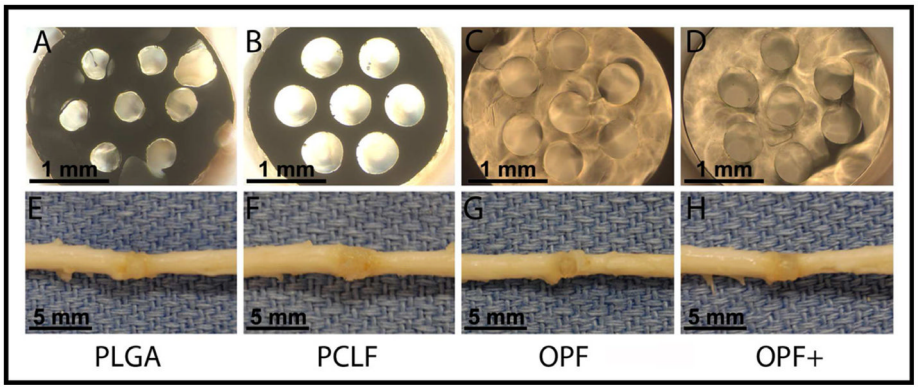

Figure 2.

Transverse view of scaffold made from PLGA (**A**), PCLF (**B**), OPF (**C**), and OPF+ (**D**) polymers under the surgical microscope showing 7 channels.

Macroscopic view of scaffold made from PLGA (**E**), PCLF (**F**), OPF (**G**), and OPF+ (**H**) polymers implanted and interacted with the cord tissues.

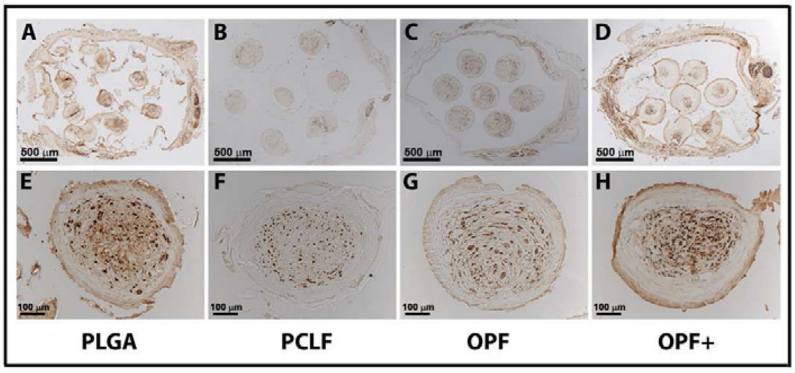

Figure 3.

NF-stained axons regenerated into the channels of scaffolds loaded with schwann cells 1 month after cord transection in rats.

Transverse section view of scaffold made from PLGA (**A,** 2/4 level), PCLF (**B,** 1/4 level), OPF (**C,** 3/4 level), and OPF+ (**D,** 3/4 level) polymers under microscope in lower magnification showing 7 channels. Transverse section view of scaffold made from PLGA (**E,** 1/4 level), PCLF (**F,** 1/4 level), OPF (**G,** 3/4 level), and OPF+ (**H,** 3/4 level) polymers under microscope in higher magnification showing a single channel.

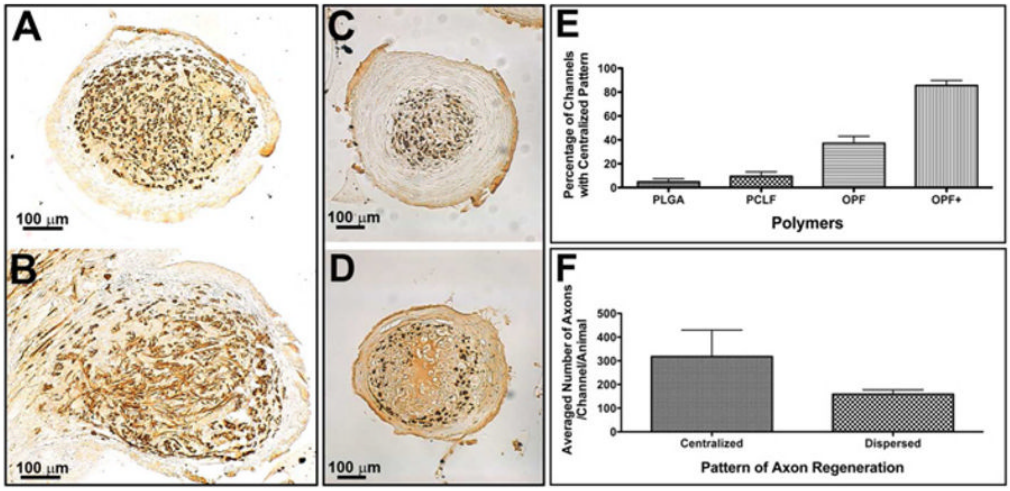

Figure 4.

Different patterns of axonal regeneration in the channels of implanted polymer scaffolds. (**A**): Well oriented axons regenerated in the channel at 2/4 level of an OPF+ polymer scaffold showing as round dots; (**B**): Poorly oriented axons regenerated in the channel at 3/4 level of an OPF+ polymer scaffold showing as rods; (**C**): Centralized pattern of axonal regeneration in the channel from an OPF+ polymer group; (**D**): Dispersed pattern of axonal regeneration in the channel from a PCLF polymer group; (**E**): The percentages of channels with centralized infiltrating pattern in each polymer group; (**F**): The averaged number of axons per channel per animal in different patterns of axonal regeneration (centralized vs. dispersed). There is a significant increase in the number of channels with the centralized pattern in OPF+ scaffolds ($P < 0.0001$) and a significantly increased number of axons associated with the central distribution ($P = 0.0268$).

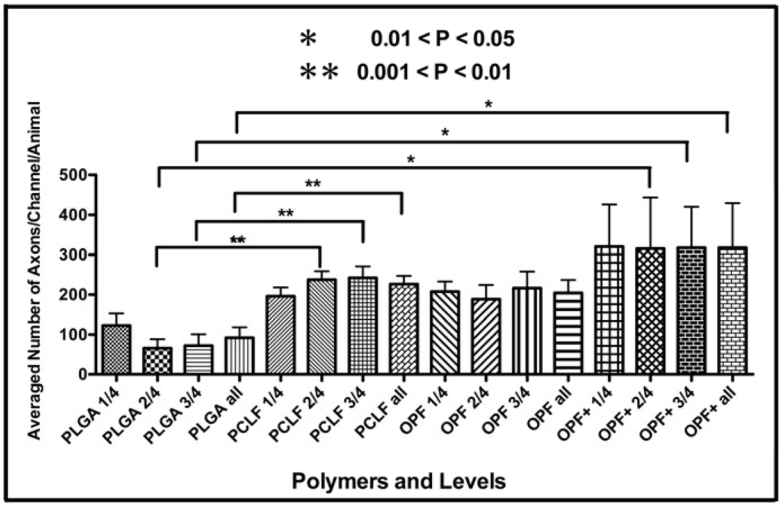

Figure 5.

Counted numbers of axons regenerated into different polymer scaffolds.

The averaged number of axon fibers was graphically shown per channel in the 1st(1/4), 2nd (2/4), 3rd (3/4) quarter and the whole length through the entire scaffold per animal after 1 month after transection of the spinal cord. Error bars represented the standard error of the mean. * 0.05 > P >0.01; ** 0.01 > P > 0.001

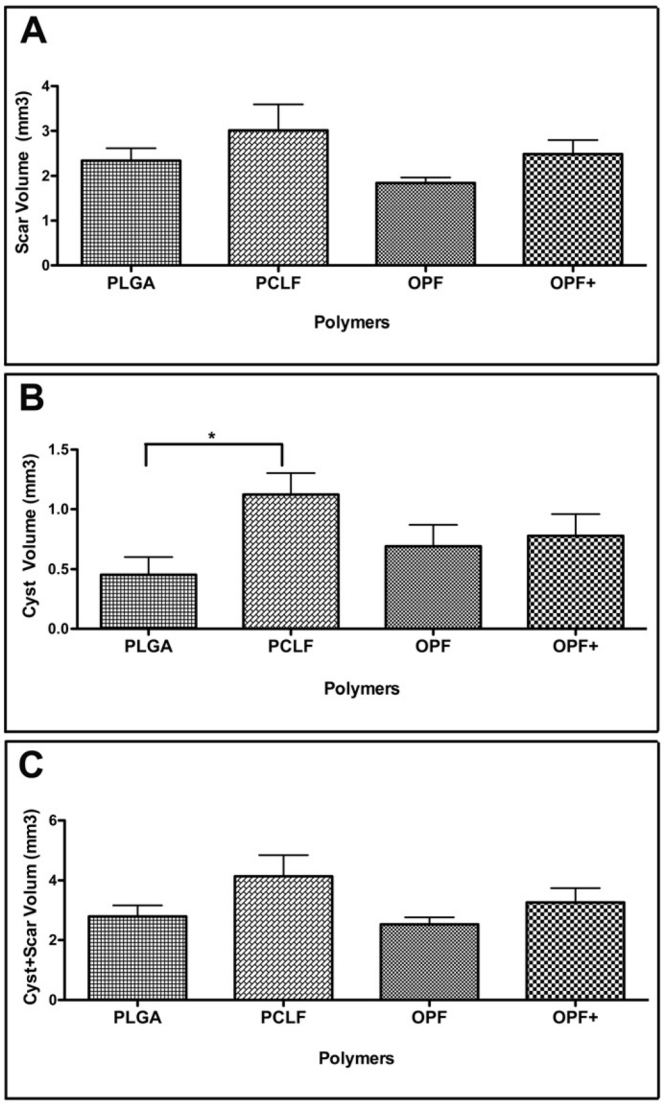

Figure 6.

Graphic representation of the scar and cyst formation in different polymer groups. (**A**): The volume of scar of the interface both rostral and caudal to the implanted scaffold; (**B**): The volume of cyst of the interface both rostral and caudal to the implanted scaffold; (**C**): The volume of combined scar and cyst both rostral and caudal to the implanted scaffold. These were assessed by the Trichrome staining of collagen fibers in the rostral interface, caudal interface and a combination of both in the transversely sectioned spinal cord. Error bar represent standard error of the mean. * $P < 0.05$.

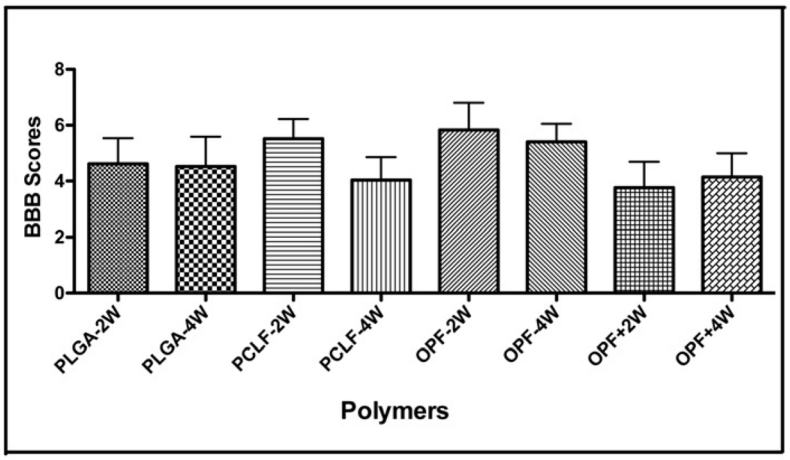

Figure 7.
Functional assessment in different polymer groups after 1 month transection. BBB scores were measured and graphically represented in different polymer groups at 2-week and 4-week intervals after 1 month transection. Error bar represent standard error of the mean.

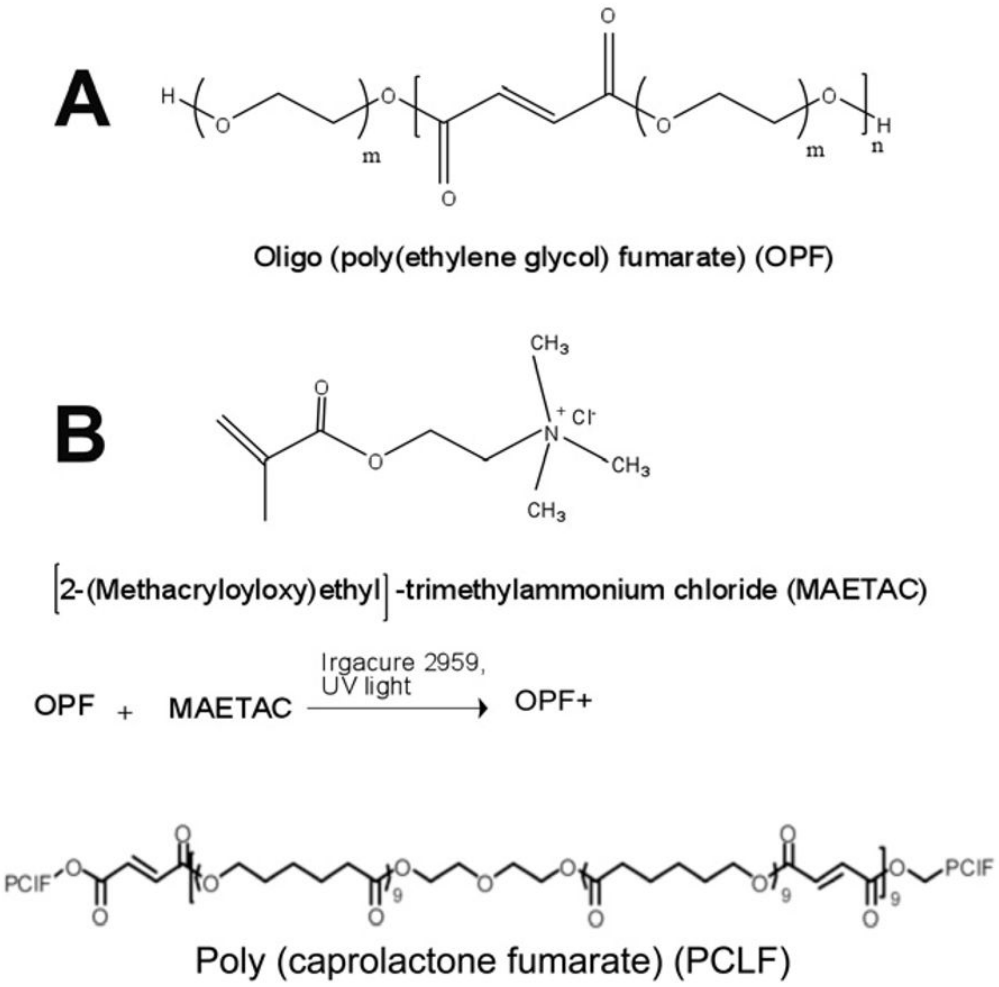

Scheme 1.

Chemical structure of oligo (polyethylene glycol) fumarate (OPF), Poly (caprolactone fumarate) (PCLF) and OPF+. The OPF (**A**), composed of repeating PEG and fumarate chains, was crosslinked with [2-(methacryloyloxy) ethyl]-trimethylammonium chloride (MAETAC) (**B**) in the presence of the photoinitiator Irgacure 2959 and ultraviolet light to form positively charged hydrogels (OPF+).